Shot Noise Suppression in Quasi-One-Dimensional Field-Effect Transistors

Alessandro Betti
Dipartimento di Ingegneria dell’Informazione: Elettronica, Informatica, Telecomunicazioni,
Università di Pisa
Gianluca Fiori
Dipartimento di Ingegneria dell’Informazione: Elettronica, Informatica, Telecomunicazioni,
Università di Pisa
Giuseppe Iannaccone
Dipartimento di Ingegneria dell’Informazione: Elettronica, Informatica, Telecomunicazioni,
Università di Pisa

A. Betti, G. Fiori, G. Iannaccone, *Shot Noise Suppression in Quasi-One-Dimensional Field-Effect Transistors*, IIEEE Transactions on Electron Devices, **56**, 9, pp.2137-2143 (2009).

Shot Noise Suppression in Quasi-One-Dimensional Field-Effect Transistors

Alessandro Betti, Gianluca Fiori, and Giuseppe Iannaccone, *Member, IEEE*

***Abstract*—We present a novel method for the evaluation of shot noise in quasi-1-D field-effect transistors, such as those based on carbon nanotubes and silicon nanowires. The method is derived by using a statistical approach within the second quantization formalism and allows the inclusion of both the effects of Pauli exclusion and Coulomb repulsion among charge carriers. This way, it extends the Landauer–Büttiker approach by explicitly including the effect of Coulomb repulsion on noise. We implement the method through the self-consistent solution of the 3-D Poisson and transport equations within the nonequilibrium Green's function framework and a Monte Carlo procedure for populating injected electron states. We show that the combined effect of Pauli and Coulomb interactions reduces shot noise in strong inversion down to 23% of the full shot noise for a gate overdrive of 0.4 V, and that neglecting the effect of Coulomb repulsion would lead to an overestimation of noise up to 180%.**

***Index Terms*—Carbon nanotube (CNT) transistors, field-effect transistors (FETs), nanowire transistors, shot noise.**

I. Introduction

IN THE past few years, huge collective effort has been directed to assess potential performance of quasi-1-D field-effect transistors (FETs) based on carbon nanotubes (CNTs) [1]–[3], silicon nanowires (SNWs) [4], and graphene nanoribbons versus the International Technology Roadmap for Semiconductors (ITRS) [5] requirements, both from an experimental and a theoretical point of view. However, attention has been focused on electrical quantities like $I_{\rm on}/I_{\rm off}$, subthreshold slope, mobility, and transconductance [6]–[8], while an accurate investigation of electrical noise has often been neglected. Although the $1/f$ noise represents the major noise source affecting CNT-FETs' performance [9], [10], the intrinsic shot noise is not only critical from analog and digital design points of view, but it can also provide relevant information regarding interactions among carriers [11]–[13], electron energy distribution [14], [15], and electron kinetics [16].

Manuscript received February 26, 2009; revised June 15, 2009. First published August 4, 2009; current version published August 21, 2009. This work was supported in part by the European Community (EC) Seventh Framework Program through the Network of Excellence NANOSIL under Contract 216171, by the European Science Foundation EUROCORES Program Fundamentals of Nanoelectronics through funds from the Consiglio Nazionale delle Ricerche, and by the EC Sixth Framework Program through Project DEWINT under Contract ERAS-CT-2003-980409. The review of this paper was arranged by Editor M. J. Deen.

The authors are with the Dipartimento di Ingegneria dell'Informazione: Elettronica, Informatica, Telecomunicazioni, Università di Pisa, 56100 Pisa, Italy (e-mail: alessandro.betti@iet.unipi.it; gfiori@mercurio.iet.unipi.it; g.iannaccone@iet.unipi.it).

Color versions of one or more of the figures in this paper are available online at http://ieeexplore.ieee.org.

Digital Object Identifier 10.1109/TED.2009.2026512

Due to the limited device dimensions, even in strong inversion, only few electrons take part to transport so that drain current fluctuations can heavily affect the device electrical behavior. Pauli and Coulomb interactions play an important role in noise analysis through fluctuations of the occupation number of injected states and fluctuations of the potential barrier along the channel.

From a numerical point of view, a self-consistent (SC) solution of the electrostatics and transport equations is mandatory in order to properly consider such effects. An analysis of this kind has been performed for example in double-gate MOSFETs [17] and in nanoscale ballistic MOSFETs [18], where a strong shot noise suppression, mostly due to Pauli exclusion principle, has been observed.

A different approach, based on quantum trajectories within the De Broglie–Bohm framework, has been instead presented in [19], where resonant tunneling diodes have been studied and heavy approximations have been adopted in order to easily consider electron–electron correlation in the many-body problem.

Actually, a complete understanding of the mechanism of suppression of shot noise in CNT and SNW-FETs is still a debated issue. Indeed, the significant suppression of current fluctuations by more than a factor of 100 obtained at a low temperature for 0.4-μm-long suspended ropes of single-wall CNTs [20] has not been supported by a comprehensive theoretical analysis. Recent experiments of shot noise in CNT-based Fabry–Perot interferometers [21] show that by including only Pauli exclusion, one is able to explain most of the dependence of shot noise on the backgate bias, but in some bias conditions, additional mechanisms of electron–electron interaction might be needed to explain the observed noise suppression. Theoretical effort has been mainly addressed to model the electrical noise in SNW-FETs, where, within a scattering approach with the limitation of excluding space-charge effects on electron transmission, Pauli exclusion reduces electrical noise in strong inversion down to 0.6% of the full value for a gate overdrive of 0.3 V [22], whereas an interesting increase of noise is observed by including electron–phonon scattering processes [23].

Here, we present a new method for computing the shot noise power spectral density in ballistic CNT and SNW-FETs based on Monte Carlo (MC) simulations of randomly injected electrons from the reservoirs. In order to consider correlations between fermions, an analytical formula for the noise power spectral density has been computed by means of a statistical approach within the second quantization formalism. The derived formula has then been implemented in the SC solution of

0018-9383/$26.00 © 2009 IEEE

Authorized licensed use limited to: UNIVERSITA PISA S ANNA. Downloaded on October 26, 2009 at 05:55 from IEEE Xplore. Restrictions apply.

the 3-D Poisson and Schrödinger equations, within the NEGF formalism.

II. Theory

The average current in a mesoscopic conductor can be expressed by means of the following Landauer's formula:

$$\langle I\rangle = \frac{e}{\pi\hbar}\int dE\left\{\mathrm{Tr}\left[\mathbf{t}^\dagger\mathbf{t}(E)\right]\left[f_S(E)-f_D(E)\right]\right\} \quad (1)$$

where $\mathbf{t}$ is the transmission amplitude matrix for states emitted from the source S and collected at the drain D, and f_S and f_D are the Fermi–Dirac statistics of S and D, respectively.

The zero-frequency noise power spectral density for a two-terminal conductor—the so-called Landauer–Büttiker noise formula—reads [24], [25]

$$S(0) = \frac{2e^2}{\pi\hbar}\int dE\left\{\left[f_S(1-f_S)+f_D(1-f_D)\right]\mathrm{Tr}[\mathbf{t}^\dagger\mathbf{t}\mathbf{t}^\dagger\mathbf{t}] + \left[f_S(1-f_D)+f_D(1-f_S)\right]\left(\mathrm{Tr}[\mathbf{t}^\dagger\mathbf{t}]-\mathrm{Tr}[\mathbf{t}^\dagger\mathbf{t}\mathbf{t}^\dagger\mathbf{t}]\right)\right\} \quad (2)$$

where $\mathbf{t}^\dagger$ is the conjugate transpose of the matrix $\mathbf{t}$. However, (2) holds only if one assumes that fluctuations of the potential profile do not occur, i.e., that Coulomb interaction between carriers is completely neglected. Actually, the potential barrier along the channel fluctuates in time since randomly injected electrons modify the height of the barrier through long-range Coulomb interaction, which, in turn, affects carriers transmission and eventually leads to the suppression of the drain current fluctuations.

In order to compute the expression of the power spectral density in the general case, we take advantage of the second quantization formalism. In particular, at zero magnetic field, the time-dependent current operator at the source can be expressed as the difference between the occupation numbers of carriers moving inward and outward the source contact in each quantum channel [24] (n^+_{Sm} and n^-_{Sm}, respectively), i.e.,

$$I(t) = \frac{e}{2\pi\hbar}\sum_{m\in S}\int dE\left[n^+_{Sm}(E,t)-n^-_{Sm}(E,t)\right] \quad (3)$$

where

$$n^+_{Sm}(E,t) = \int d(\hbar\omega)a^+_{Sm}(E)a_{Sm}(E+\hbar\omega)e^{-i\omega t}$$
$$n^-_{Sm}(E,t) = \int d(\hbar\omega)b^+_{Sm}(E)b_{Sm}(E+\hbar\omega)e^{-i\omega t}. \quad (4)$$

The operators $a^\dagger_{Sm}(E)$ and $a_{Sm}(E)$ create and annihilate, respectively, incident electrons in the source lead with total energy E in the transverse channel m. In the same way, the creation $b^\dagger_{Sm}(E)$ and annihilation $b_{Sm}(E)$ operators refer to the electrons in the source lead for outgoing states. For the CNT case, the channel index m runs over all the transverse modes and different spins, whereas for SNW, it also runs along the six minima of the conduction band in the $\mathbf{k}$ space. In addition, the operators a_S and b_S are related through the following unitary transformation:

$$b_{Sm}(E) = \sum_{\alpha=S,D}\sum_{n\in\alpha}^{N_\alpha}\mathbf{s}_{S\alpha;mn}(E)a_{\alpha n}(E) \quad (5)$$

where the scattering matrix $\mathbf{s}$ has dimensions $(N_S+N_D)\times(N_S+N_D)$, and N_S and N_D are the number of quantum channels in the source and drain contacts, respectively. In the following, time dependence will be neglected, since we are interested to the zero frequency case.

If $|\sigma\rangle$ is a many-particle (antisymmetrical) state, the occupation number $\sigma_{\alpha m}(E)$ in the reservoir α ($\alpha = S, D$) in the channel m can be either 0 or 1 and can be expressed as $\sigma_{\alpha m}(E) = \langle a^\dagger_{\alpha m}(E)a_{\alpha m}(E)\rangle_\sigma$. Since we are interested on current fluctuations, we need to consider an ensemble of many electrons states $\{|\sigma_1\rangle, |\sigma_2\rangle, |\sigma_3\rangle, \ldots, |\sigma_N\rangle\}$ and to compute statistical averages $\langle\,\rangle_s$. By neglecting correlation between electron states corresponding to different energy or injected from different reservoirs, the statistical average of $\sigma_{\alpha m}(E)$ reads

$$\langle\sigma_{\alpha m}(E)\rangle_s = \left\langle\left\langle a^\dagger_{\alpha m}(E)a_{\alpha m}(E)\right\rangle_\sigma\right\rangle_s = f_\alpha(E). \quad (6)$$

In the following, we identify $\langle\langle\,\rangle_\sigma\rangle_s$ with $\langle\,\rangle$. By means of (5), we obtain the mean current as follows:

$$\langle I\rangle = \frac{e}{2\pi\hbar}\int dE\left\{\sum_{n\in S}\left\langle\left[\mathbf{t}^\dagger\mathbf{t}(E)\right]_{nn}\sigma_{Sn}(E)\right\rangle_s - \sum_{k\in D}\left\langle\left[\mathbf{t}'^\dagger\mathbf{t}'(E)\right]_{kk}\sigma_{Dk}(E)\right\rangle_s\right\} \quad (7)$$

where $\mathbf{t}'$ is the drain-to-source transmission amplitude matrix [26]. Since $\sigma^2_{\alpha m} = \sigma_{\alpha m}\ \ \forall m\in\alpha$, and by exploiting the unitarity of the scattering matrix, the mean squared current fluctuation for unit of energy can be expressed as

$$\begin{aligned}\frac{\mathrm{var}(I)}{\Delta E} =& \left(\frac{e}{h}\right)^2\int dE\sum_{\alpha=S,D}\sum_{l\in\alpha}\left\langle[\tilde{\mathbf{t}}]_{\alpha;ll}\left(1-[\tilde{\mathbf{t}}]_{\alpha;ll}\right)\sigma_{\alpha l}\right\rangle_s \\ &- \left(\frac{e}{h}\right)^2\int dE\sum_{\alpha=S,D}\sum_{\substack{l,p\in\alpha\\ l\neq p}}\left\langle[\tilde{\mathbf{t}}]_{\alpha;lp}[\tilde{\mathbf{t}}]_{\alpha;pl}\sigma_{\alpha l}\sigma_{\alpha p}\right\rangle_s \\ &- 2\left(\frac{e}{h}\right)^2\int dE\sum_{k\in D}\sum_{p\in S}\left\langle[\mathbf{t}'^\dagger\mathbf{r}]_{kp}[\mathbf{r}^\dagger\mathbf{t}']_{pk}\sigma_{Dk}\sigma_{Sp}\right\rangle_s \\ &+ \frac{1}{\Delta E}\mathrm{var}\left\{\frac{e}{h}\int dE\left(\sum_{n\in S}[\tilde{\mathbf{t}}]_{S;nn}\sigma_{Sn} - \sum_{k\in D}[\tilde{\mathbf{t}}]_{D;kk}\sigma_{Dk}\right)\right\}\end{aligned} \quad (8)$$

where $[\tilde{\mathbf{t}}]$ is defined as

$$[\tilde{\mathbf{t}}]_{\alpha;lp} = \begin{cases}[\mathbf{t}^\dagger\mathbf{t}]_{lp}, & \text{if } \alpha = S\\ [\mathbf{t}'^\dagger\mathbf{t}']_{lp}, & \text{if } \alpha = D\end{cases}$$

and $\mathbf{r}$ is the reflection amplitude matrix [26]. ΔE is our energy step of choice, i.e., the minimum energy separation between injected states.

Equation (8) is expressed as the sum of four terms, with the first, second, and third terms corresponding to the partition noise contribution. In particular, the first term is strictly related to the quantum uncertainty of the transmission process and disappears in the classical limit; the second term is associated to the correlation between transmitted states coming from the same reservoir; the third term is related to the correlation

Authorized licensed use limited to: UNIVERSITA PISA S ANNA. Downloaded on October 26, 2009 at 05:55 from IEEE Xplore. Restrictions apply.

between transmitted and reflected states in the source lead; the minus sign in the second and third terms is due to exchange pairings, because of the fermionic nature of the electrons. In particular, the second and the third terms provide physical insights on exchange interference effects [27]. Finally, the last term represents the injection noise obtained as the variance computed on the ensemble of current samples.

According to *Milatz's Theorem* [28], the noise power spectral density in the zero frequency limit can be computed as $S(0) = \lim_{f\to 0} S(f) = \lim_{\nu\to 0}[2/\nu \cdot \mathrm{var}(I)]$, where ν is the injection rate, which can be expressed as

$$\nu = \Delta E/(2\pi\hbar). \tag{9}$$

Eventually, the power spectral density of shot noise at zero frequency can be expressed as

$$S(0) = \lim_{\nu\to 0}\frac{2}{\nu}\mathrm{var}(I) = \lim_{\Delta E\to 0} 4\pi\hbar\frac{\mathrm{var}(I)}{\Delta E}. \tag{10}$$

It is worth noticing that (10) and (8) are not equivalent to Landauer–Büttiker's formula (2) since in (8), the transmission $(\mathbf{t}, \mathbf{t}')$ and reflection $(\mathbf{r})$ matrices are expressed as functions of the statistics of the occupation of injected states from both contacts. This way, we are able to consider the fluctuation in time of the conduction and valence band edge profiles produced by the random injection through long-range Coulomb repulsion, providing a further source of noise suppression not included in (2).

Indeed, from an analytical point of view, (8) and (10) reduce to (2) when transmission and reflection do not depend, through Coulomb interaction, on random occupation numbers of injected states: in that case, we can take the terms related to transmission and reflection out of the statistical averages in (8). By means of (6) and exploiting $\langle\sigma_{\alpha l}(E)\sigma_{\beta n}(E')\rangle_s = f_\alpha(E)f_\beta(E') + \delta(E-E')\delta_{\alpha\beta}\delta_{ln}[f_\alpha(E) - f_\alpha(E)f_\beta(E')]$, the fourth term in (8) becomes

$$\left(\frac{e}{h}\right)^2 \int dE \sum_{n\in S}\left[\mathbf{t}^\dagger\mathbf{t}(E)\right]^2_{nn} f_S(E)\left[1-f_S(E)\right] + \left(\frac{e}{h}\right)^2 \int dE \sum_{k\in D}\left[\mathbf{t}\mathbf{t}^\dagger(E)\right]^2_{kk} f_D(E)\left[1-f_D(E)\right] \tag{11}$$

since at zero magnetic field, $\mathbf{t}'^\dagger\mathbf{t}' = \mathbf{t}\mathbf{t}^\dagger$. The terms $\delta(E-E')$, $\delta_{\alpha\beta}$, and δ_{ln} represent the Kronecker delta. Taking advantage of $\sum_{k\in D}\sum_{p\in S}[\mathbf{t}'^\dagger\mathbf{r}]_{kp}[\mathbf{r}^\dagger\mathbf{t}']_{pk} = \mathrm{Tr}[\mathbf{t}^\dagger\mathbf{t}] - \mathrm{Tr}[\mathbf{t}^\dagger\mathbf{t}\mathbf{t}^\dagger\mathbf{t}]$, $S(0)$ becomes

$$\begin{aligned} S(0) &= \lim_{\Delta E\to 0} 4\pi\hbar\frac{\mathrm{var}(I)}{\Delta E} \\ &= \frac{2e^2}{\pi\hbar}\int dE\Big\{\left[f_S(1-f_S) + f_D(1-f_D)\right]\mathrm{Tr}\left[\mathbf{t}^\dagger\mathbf{t}\mathbf{t}^\dagger\mathbf{t}\right] \\ &\quad + \left[f_S(1-f_D) + f_D(1-f_S)\right] \\ &\quad \times \left(\mathrm{Tr}[\mathbf{t}^\dagger\mathbf{t}] - \mathrm{Tr}[\mathbf{t}^\dagger\mathbf{t}\mathbf{t}^\dagger\mathbf{t}]\right)\Big\} \end{aligned} \tag{12}$$

which is Landauer–Büttiker's formula (2).

Let us now point out that (10) would also simplify when identical and independent injected modes from the reservoirs are considered. In this case, $\mathbf{t}$, $\mathbf{t}'$, and $\mathbf{r}$ are all diagonals so that the second term in (8) becomes negligible. By exploiting the reversal time symmetry ($\mathbf{t}' = \mathbf{t}^{\mathbf{t}}$, where $\mathbf{t}^{\mathbf{t}}$ is the transpose of $\mathbf{t}$) and the unitarity of the scattering matrix, the power spectral density becomes

$$\begin{aligned} S(0) = \frac{e^2}{\pi\hbar}\Bigg\{ &\int dE \sum_{\alpha=S,D}\sum_{l\in\alpha}\left\langle[\tilde{\mathbf{t}}]_{\alpha;ll}\left(1-[\tilde{\mathbf{t}}]_{\alpha;ll}\right)\sigma_{\alpha l}\right\rangle_s \\ &- 2\int dE\sum_{l\in S}\left\langle[\tilde{\mathbf{t}}]_{S;ll}\left(1-[\tilde{\mathbf{t}}]_{S;ll}\right)\sigma_{Dl}\sigma_{Sl}\right\rangle_s \\ &+ \frac{1}{\Delta E}\mathrm{var}\left[\int dE\left(\sum_{n\in S}[\tilde{\mathbf{t}}]_{S;nn}\sigma_{Sn} - \sum_{k\in D}[\tilde{\mathbf{t}}]_{D;kk}\sigma_{Dk}\right)\right]\Bigg\}. \end{aligned} \tag{13}$$

III. Simulation Methodology

In order to properly include the effect of Coulomb interaction, we self-consistently solve the 3-D Poisson equation, imposing Dirichlet boundary conditions in correspondence to the metal gates and null Neumann boundary conditions on the ungated surfaces, which define the 3-D domain. Within an SC scheme, the 3-D Poisson equation is coupled with the Schrödinger equation with open-boundary conditions, within the nonequilibrium Green's function (NEGF) formalism, which has been implemented in our in-house open-source simulator *NanoTCAD ViDES* [29]. In particular, the 3-D Poisson equation reads

$$\nabla\left(\epsilon\nabla\phi(\vec{r})\right) = -\left(\rho(\vec{r}) + \rho_{\mathrm{fix}}(\vec{r})\right) \tag{14}$$

where ϕ is the electrostatic potential, ρ_{fix} is the fixed charge that accounts for ionized impurities in the doped regions, while ρ is the charge density per unit volume, i.e.,

$$\begin{aligned} \rho(\vec{r}) = -e\int_{E_i}^{+\infty} dE \sum_{\alpha=S,D}\sum_{n\in\alpha}\mathrm{DOS}_{\alpha n}(\vec{r},E)\sigma_{\alpha n}(E) \\ + e\int_{-\infty}^{E_i} dE\sum_{\alpha=S,D}\sum_{n\in\alpha}\mathrm{DOS}_{\alpha n}(\vec{r},E)\left[1-\sigma_{\alpha n}(E)\right] \end{aligned} \tag{15}$$

where E_i is the midgap potential, $\mathrm{DOS}_{\alpha n}(\vec{r},E)$ is the local density of states associated to channel n injected from contact α, and $\vec{r}$ is the 3-D spatial coordinate.

From a numerical point of view, in order to model the stochastic injection of electrons from the contacts, a statistical simulation on an ensemble of random configurations of injected electron states from both contacts has been performed. In particular, we have uniformly discretized with step ΔE the whole energy range of integration [see (8) and (15)]. Each random

Authorized licensed use limited to: UNIVERSITA PISA S ANNA. Downloaded on October 26, 2009 at 05:55 from IEEE Xplore. Restrictions apply.

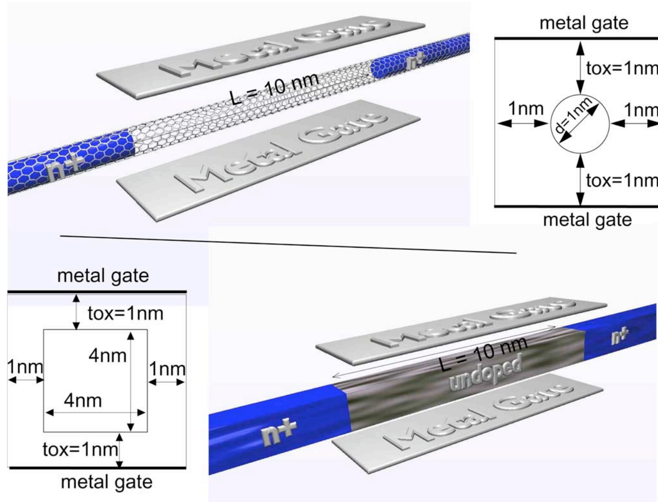

Fig. 1. Three-dimensional structures and transversal cross sections of the simulated (top) CNT and (bottom) SNW-FETs.

injection configuration has been obtained by extracting a random number r uniformly distributed between 0 and 1 for each state represented by energy E, reservoir α, and quantum channel n. The state is occupied if r is smaller than the Fermi–Dirac factor, i.e., $\sigma_{Sn}(E)[\sigma_{Dn}(E)]$ is 1 for $r < f_S(E)[f_D(E)]$, and 0 otherwise.

SC simulations for a given actual random statistics in the source and drain contacts have been performed, and at convergence, the transmission $(\mathbf{t}, \mathbf{t}')$ and reflection $(\mathbf{r})$ matrices have been computed, obtaining an element of the ensemble. In particular, for an actual electron distribution in the contacts, the Schrödinger equation is solved in order to obtain the spatial charge distribution (15) along the channel. Then, the latter is included in (14), and the electrostatic potential is then computed, and once convergence of the NEGF–Poisson iteration scheme is achieved, the scattering matrix is evaluated, and a new sample to be added to the noise ensemble is obtained. Finally, the power spectral density $S(0)$ can be extracted by means of (8) and (10). From a computational point of view, we have verified that $S(0)$ computed on a record of 500 samples, using the energy step $\Delta E = 5 \times 10^{-4}$ eV, represents a good tradeoff between computational cost and accuracy of results [30].

Let us mention the fact that our approach is based on a mean field approximation of the Coulomb interaction, and that, therefore, the exchange term is not included. In the following, we will refer to SC simulations when the Poisson–Schrödinger equations are solved considering f_S and f_D in (15), while we refer to SC-MC simulations when statistical simulations with random occupations $\sigma_{Sn}(E)$ and $\sigma_{Dn}(E)$ inserted in (15) are used. SC-MC simulations of randomly injected electrons allow us to consider both the effects of Pauli and Coulomb interactions on noise. As a test, we have verified that if we perform MC simulations, keeping the potential profile along the channel fixed and exploiting the one obtained by means of SC simulation, the noise power spectrum computed this way reduces to Landauer–Büttiker's limit (2), as already proved in an analytical way (12): we refer to such simulations as non-SC-MC (non-SC-MC) simulations.

IV. Simulation Results

A. Considered Devices

The simulated device structures are depicted in Fig. 1. We consider a (13,0) CNT embedded in SiO_2 with an oxide thickness equal to 1 nm, an undoped channel of 10 nm, and 10-nm-long n-doped CNT extensions, with a molar fraction $f = 5 \times 10^{-3}$. The SNWT has an oxide thickness $t_{\rm ox}$ equal to 1 nm, and the channel length L is 10 nm. The channel is undoped, and the source and drain extensions (10 nm long) are doped with $N_D = 10^{20}$ cm^{-3}. The device cross section is 4×4 nm^2. A p_z-orbital tight-binding Hamiltonian has been assumed for CNTs [31], [32], whereas an effective mass approximation has been considered for SNWTs [33], [34] by means of an adiabatic decoupling in a set of 2-D equations in the transversal plane and in a set of 1-D equations in the longitudinal direction for each 1-D subband.

For both devices, we have developed a quantum fully ballistic transport model with semiinfinite extensions at their ends. A mode space approach has been adopted since only the lowest subbands take part to transport: we have verified that four modes are enough to compute the mean current both in the ohmic and saturation regions. All calculations have been performed at the temperature $T = 300$ K.

B. DC Characteristics

In Fig. 2, the transfer characteristics for different drain-to-source biases V_{DS} computed performing SC and SC-MC simulations are plotted as a function of the gate overdrive V_{GS}–$V_{\rm th}$ in the logarithmic scale, both for CNT and SNW devices. In particular, the threshold voltage $V_{\rm th}$ for the CNT-FET at $V_{DS} =$ 0.05 and 0.5 V is 0.43 V, whereas we obtain $V_{\rm th} = 0.13$ V for $V_{DS} = 0.05$ V and 0.5 V for the SNW-FET. As can be noted, SC and SC-MC simulations give practically the same results for CNT-FET, except in the subthreshold region where an interesting rectifying effect of the statistics emerges in the MC simulations for a drain-to-source bias $V_{DS} = 0.5$ V.

Instead, the rectifying effect is larger for SNW-FET, and differences up to 30% between the drain current $\langle I \rangle$ computed by means of SC-MC and SC simulations can be also observed in the above threshold regime. In particular, for a gate voltage $V_{GS} = 0.5$ V and a drain-to-source voltage $V_{DS} = 0.5$ V, the drain current $\langle I \rangle$ holds 2.42×10^{-5} A, applying (7), and 1.89×10^{-5} A, applying Landauer's formula (1). The current in the CNT-FET transfer characteristics increases for negative gate voltages due to the interband tunneling. Indeed, the larger the negative gate voltage, the higher the number of electrons that tunnel from bound states in the valence band to the drain, leaving positive charge in the channel, which eventually lowers the barrier and increases the off current [35].

In the inset of Fig. 2, the average number of electrons inside the channel of a CNT and SNW-FET for two different biases $V_{DS} = 0.5$ and 0.05 V is shown. As can be seen, only very few electrons contribute to transport at any given instant, which requires us to attentively evaluate the sensitivity of such devices to charge fluctuations: the smaller the drain-to-source voltage, the larger the average number of electrons in the

Authorized licensed use limited to: UNIVERSITA PISA S ANNA. Downloaded on October 26, 2009 at 05:55 from IEEE Xplore. Restrictions apply.

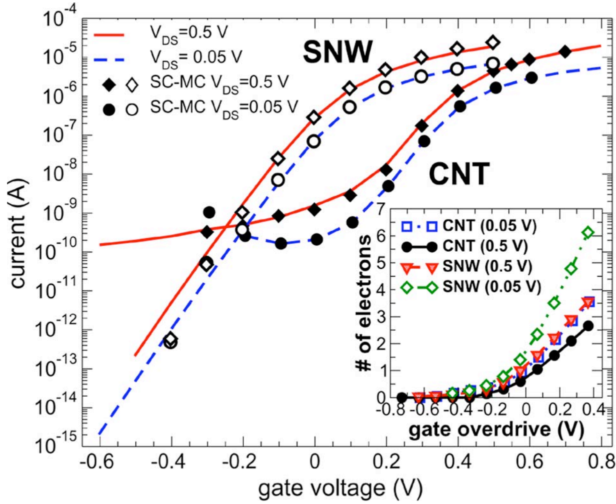

Fig. 2. Transfer characteristics computed for $V_{DS} = 0.5$ and 0.05 V, obtained by SC-MC and SC simulations, for CNT and SNW-FET. Full dots refer to CNT, and empty dots refer to SNW. Inset: average number of electrons in the CNT-FET and SNW-FET channels, evaluated for $V_{DS} = 0.5$ and 0.05 V.

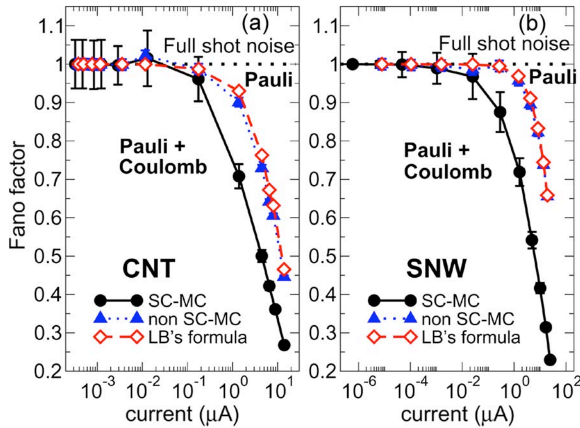

Fig. 3. Fano factor as a function of the drain current $\langle I \rangle$ for (a) CNT and (b) SNW-FETs for $V_{DS} = 0.5$ V. Solid line refers to the Fano factor F obtained by means of SC-MC simulations, dashed line (diamonds) by means of applying (2), and dotted line (triangles) by means of non-SC-MC simulations.

channel, since, for low V_{DS}, carriers are injected from both contacts.

C. Noise

Let us now focus our attention on the Fano factor F, which is defined as the ratio of the computed noise power spectral density $S(0)$ and the full shot noise $2e\langle I \rangle$, $F = S(0)/(2e\langle I \rangle)$. In Fig. 3, the Fano factor for both CNT-FETs and SNW-FETs is shown for $V_{DS} = 0.5$ V as a function of drain-to-source current $\langle I \rangle$.

Let us separately discuss the effects of Pauli exclusion alone and the concurrent Pauli and Coulomb interactions. Triangles in Fig. 3 refer to F, computed by means of non-SC-MC simulations on 10^4 samples, while diamonds refer to the results obtained by means of Landauer–Büttiker's formula, applying (2). As expected, the two approaches give the same results for both structures. Solid lines refer to $S(0)$, computed by means of (8) and (10) and SC-MC simulations, i.e., Pauli and Coulomb interactions simultaneously taken into account.

In the subthreshold regime ($\langle I \rangle < 10^{-9}$ A), drain current noise is very close to the full shot noise, since electron–electron correlations are negligible due to the very small amount of mobile charge in the channel.

From the point of view of (2), for energies larger than the top of the barrier, we have $f_D(E) \ll f_S(E) \ll 1$, and the integrand in (2) reduces to $\mathrm{Tr}[\mathbf{t}^\dagger \mathbf{t}(E)] f_S(E)$. Instead, for energies smaller than the high potential profile along the channel, $[\mathbf{t}^\dagger \mathbf{t}(E)]_{nm} \ll 1 \ \forall n, m \in S$ so that we can neglect $\mathrm{Tr}[\mathbf{t}^\dagger \mathbf{t} \mathbf{t}^\dagger \mathbf{t}]$ in (2), with respect to $\mathrm{Tr}[\mathbf{t}^\dagger \mathbf{t}]$. Since $f_D(E) \ll f_S(E)$, the integrand in (2) still reduces to $\mathrm{Tr}[\mathbf{t}^\dagger \mathbf{t}(E)] f_S(E)$. The Fano factor then becomes

$$F = \frac{S(0)}{2e\langle I \rangle} \approx \frac{\frac{2e^2}{\pi\hbar} \int dE \, \mathrm{Tr}\left[\mathbf{t}^\dagger \mathbf{t}(E)\right] f_S(E)}{2e\frac{e}{\pi\hbar} \int dE \, \mathrm{Tr}\left[\mathbf{t}^\dagger \mathbf{t}(E)\right] f_S(E)} = 1. \tag{16}$$

In the strong inversion regime instead ($\langle I \rangle > 10^{-6}$ A), the noise is strongly suppressed with respect to the full shot value. In particular, for a SNW-FET, at $\langle I \rangle \approx 2.4 \times 10^{-5}$ A ($V_{GS} - V_{\mathrm{th}} \approx 0.4$ V), combined Pauli and Coulomb interactions suppress shot noise down to 23% of the full shot noise value, with a significant reduction with respect to the value predicted without including space charge effects as in [22], while for CNT-FET, the Fano factor is equal to 0.27 at $\langle I \rangle \approx 1.4 \times 10^{-5}$ A ($V_{GS} - V_{\mathrm{th}} \approx 0.3$ V). Indeed, an injected electron tends to increase the potential barrier along the channel, leading to a reduction of the space charge and to a suppression of charge fluctuation. Note that by considering only Pauli exclusion principle, we would overestimate the shot noise by 180% for SNWT ($\langle I \rangle \approx 2.4 \times 10^{-5}$ A) and by 70% for CNT-FET ($\langle I \rangle \approx 1.4 \times 10^{-5}$ A).

D. Shot Noise Versus Thermal Channel Noise

According to the classical approach for the formulation of drain current noise, channel noise is typically described in terms of a "modified" thermal noise, as $S(0) = \gamma S_T$, where $S_T = 4K_B T g_{d0}$ is the thermal noise power spectrum at zero drain-to-source bias V_{DS}, k_B is the Boltzmann constant, γ is a correction parameter, and $g_{d0} = (\partial \langle I \rangle / \partial V_{DS})_{V_{DS}=0}$ is the source-to-drain conductance at zero V_{DS}.

Although the classical formulation accurately predicts drain current noise in long-channel MOSFETs, where γ is equal to 1 in the ohmic region and 2/3 in saturation [28], it underestimates noise in short-channel devices. In particular, experimental evidences [36] of an excess noise in short-channel MOSFET have been explained in terms of the limited number of scattering events inside the channel, which is ineffective in suppressing the nonequilibrium noise component [37], or in terms of a revised classical formulation by considering short-channel effects, such as the carrier heating effect above the lattice temperature [38].

Actually, it can clearly be seen that nonequilibrium transport easily provides $\gamma > 1$, and that the cause of $\gamma > 1$ is simply due to the fact that channel noise can be more properly interpreted as shot noise. For example, in the particular case of ballistic transport considered here, we can plot γ as $S(0)/S_T$ as a function of the gate voltage in Fig. 4(c). As can be seen, values

Authorized licensed use limited to: UNIVERSITA PISA S ANNA. Downloaded on October 26, 2009 at 05:55 from IEEE Xplore. Restrictions apply.

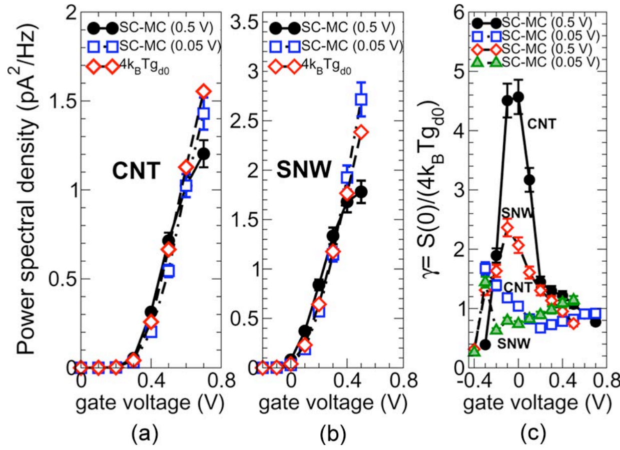

Fig. 4. Noise power spectral density obtained by SC-MC simulations and thermal noise spectral density as functions of the gate voltage for (a) CNT-FETs and (b) SNW-FETs: the considered drain-to-source biases ($V_{DS} =$ 0.5 and 0.05 V) are shown in brackets. (c) Ratio between the noise power obtained by SC-MC simulations and the thermal noise density as a function of the gate voltage. g_{d0} is the conductance evaluated for $V_{DS} = 0$ V : $g_{d0} = (\partial\langle I\rangle/\partial V_{DS})_{V_{DS}=0}$.

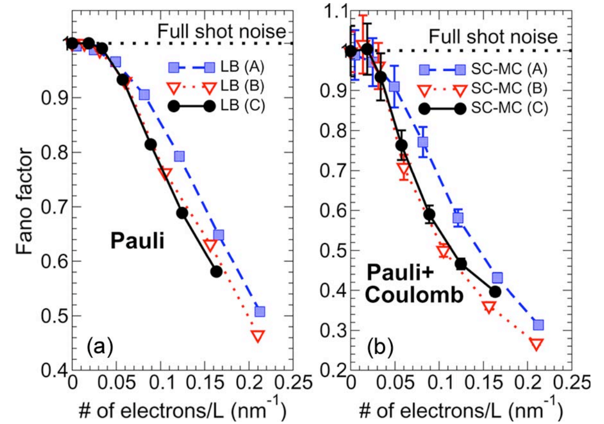

Fig. 5. Fano factor as a function of the average number of electrons inside the channel per unit length for three different (13, 0) CNT-FETs: (A) $t_{\rm ox} = 1$ nm and $L = 6$ nm; (B) $t_{\rm ox} = 1$ nm and $L = 10$ nm; and (C) $t_{\rm ox} = 2$ nm and $L = 10$ nm. (a) Only the effect of the Pauli principle is shown (2). (b) Effect of both Pauli and Coulomb interactions is considered. The drain-to-source bias V_{DS} is 0.5 V.

of γ larger than 1 can easily be observed in weak and strong inversion. The strange behavior of γ as a function of the gate voltage is simply due to the fact that one uses an inadequate model (thermal noise) corrected with the γ parameter to describe a qualitatively different type of noise, i.e., shot noise.

E. Effect of Scaling on Noise

Let us now discuss the effect of scaling on noise, focusing our attention on a (13, 0) CNT-FET. One would expect that an increase in the oxide thickness would reduce the screening induced by the metallic gate so that the Coulomb interaction would be expected to produce a larger noise suppression. For example, in the limit of a multimode ballistic conductor without a gate contact, significant suppression of about two orders of magnitude with respect to the full shot value has been shown by Bulashenko and Rubí [39].

However, Bulashenko and Rubí [39] exploit a semiclassical approach, assuming a large number of modes and the conservation of transversal momentum, i.e., the role of the transversal electric field induced by the gate voltage is completely neglected. In our case, only four modes contribute to transport, while the top and bottom gates of the simulated devices partially screen the electrostatic repulsion induced by the space charge in the channel on each injected electron so that a smaller noise suppression than the one achieved in [39] can be expected.

The Fano factor as a function of the average number of electrons inside the channel for unit length, computed by means of SC simulation and applying (2), for three CNTs with different oxide thicknesses $t_{\rm ox}$ and channel lengths L is shown in Fig. 5(a): it shows results for CNT with $t_{\rm ox} = 1$ nm and $L = 6$ nm (A), CNT with $t_{\rm ox} = 1$ nm and $L = 10$ nm (B), and CNT with $t_{\rm ox} = 2$ nm and $L = 10$ nm (C). Fig. 5(b) shows the Fano factor computed by performing SC-MC simulations and applying (8) and (10). As can be seen, if the Fano factor is plotted as a function of the number of electrons per unit length, as in Fig. 5, curves are very close to one another, and effects of scaling are predictable.

V. Conclusion

We have developed a novel and general approach to study shot noise in nanoscale quasi-1-D FETs, such as CNT-FETs and SNW-FETs. Our first important result is the derivation of an analytical formula for the noise power spectral density that exploits a statistical approach and the second quantization formalism. Our formula extends the validity of the Landauer–Büttiker noise formula (2) to also include Coulomb repulsion among electrons. From a quantitative point of view, this is very important since we show that by using only the Landauer–Büttiker noise formula, one can overestimate shot noise by as much as 180%. The second important result is the implementation of the method in a computational code, based on the 3-D SC solution of Poisson and Schrödinger equations with the NEGF formalism, and on MC simulations over a large ensemble of occurrences, with random occupation of electronic states coming in from the reservoirs. As a final note, we show that scaling of ballistic 1-D FETs is expected to weakly affect drain current fluctuations, even in the degenerate injection limit.

References

[1] R. Martel, T. Schmidt, H. R. Shea, T. Hertel, and P. Avouris, "Single- and multi-wall carbon nanotube field-effect transistors," *Appl. Phys. Lett.*, vol. 73, no. 17, pp. 2447–2449, Oct. 1998.

[2] J. Guo, A. Javey, H. Dai, and M. Lundstrom, "Performance analysis and design optimization of near ballistic carbon nanotube field-effect transistors," in *IEDM Tech. Dig.*, 2004, pp. 703–706.

[3] N. Neophytou, S. Ahmed, and G. Klimeck, "Non-equilibrium Green's function (NEGF) simulation of metallic carbon nanotubes including vacancy defects," *J. Comput. Electron.*, vol. 6, no. 1–3, pp. 317–320, Sep. 2007.

[4] Y. Cui, Z. Zhong, D. Wang, W. U. Wang, and C. M. Lieber, "High performance silicon nanowire field effect transistors," *Nano Lett.*, vol. 3, no. 2, pp. 149–152, Jan. 2003.

[5] *International Technology Roadmap for Semiconductors*. [Online]. Available: http://public.itrs.net/

Authorized licensed use limited to: UNIVERSITA PISA S ANNA. Downloaded on October 26, 2009 at 05:55 from IEEE Xplore. Restrictions apply.

[6] T. D. Yuzvinsky, W. Mickelson, S. Aloni, G. E. Begtrup, A. Kis, and A. Zettl, "Shrinking a carbon nanotube," *Nano Lett.*, vol. 6, no. 12, pp. 2718–2722, Dec. 2006.
[7] V. Perebeinos, J. Tersoff, and P. Avouris, "Mobility in semiconducting carbon nanotubes at finite carrier density," *Nano Lett.*, vol. 6, no. 2, pp. 205–208, Feb. 2006.
[8] J. Knoch and J. Appenzeller, "Tunneling phenomena in carbon nanotube field-effect transistors," *Phys. Stat. Sol. (A)*, vol. 205, no. 4, pp. 679–694, 2008.
[9] Y. M. Lin, J. Appenzeller, J. Knoch, Z. Chen, and P. Avouris, "Low-frequency current fluctuations in individual semiconducting single-wall carbon nanotubes," *Nano Lett.*, vol. 6, no. 5, pp. 930–936, May 2006.
[10] J. Appenzeller, Y.-M. Lin, J. Knoch, Z. Chen, and P. Avouris, "1/f noise in carbon nanotubes devices—On the impact of contacts and device geometry," *IEEE Trans. Nanotechnol.*, vol. 6, no. 3, pp. 368–373, May 2007.
[11] G. Iannaccone, M. Macucci, and B. Pellegrini, "Shot noise in resonant-tunneling structures," *Phys. Rev. B, Condens. Matter*, vol. 55, no. 7, pp. 4539–4550, 1997.
[12] G. Iannaccone, G. Lombardi, M. Macucci, and B. Pellegrini, "Enhanced shot noise in resonant tunneling: Theory and experiment," *Phys. Rev. Lett.*, vol. 80, no. 5, pp. 1054–1057, Feb. 1998.
[13] Y. M. Blanter and M. Bütttiker, "Transition from sub-Poissonian to super-Poissonian shot noise in resonant quantum wells," *Phys. Rev. B, Condens. Matter*, vol. 59, no. 15, pp. 10 217–10 226, Apr. 1999.
[14] T. Gramespacher and M. Büttiker, "Local densities, distribution functions, and wave-function correlations for spatially resolved shot noise at nanocontacts," *Phys. Rev. B, Condens. Matter*, vol. 60, no. 4, pp. 2375–2390, Feb. 1999.
[15] O. M. Bulashenko and J. M. Rubí, "Shot noise as a tool to probe an electron energy distribution," *Phys. E*, vol. 12, no. 1, pp. 857–860, Jan. 2002.
[16] R. Landauer, "Condensed-matter physics: The noise is the signal," *Nature*, vol. 392, no. 6677, pp. 658–659, Apr. 1998.
[17] Y. Naveh, A. N. Korotkov, and K. K. Likharev, "Shot-noise suppression in multimode ballistic Fermi conductors," *Phys. Rev. B, Condens. Matter*, vol. 60, no. 4, pp. R2 169–R2 172, Jul. 1999.
[18] G. Iannaccone, "Analytical and numerical investigation of noise in nanoscale ballistic field effect transistors," *J. Comput. Electron.*, vol. 3, no. 3/4, pp. 199–202, Oct. 2004.
[19] X. Oriols, A. Trois, and G. Blouin, "Self-consistent simulation of quantum shot noise in nanoscale electron devices," *Appl. Phys. Lett.*, vol. 85, no. 16, pp. 3596–3598, Oct. 2004.
[20] P.-E. Roche, M. Kociak, S. Guéron, A. Kasumov, B. Reulet, and H. Bouchiat, "Very low shot noise in carbon nanotubes," *Eur. Phys. J. B*, vol. 28, no. 2, pp. 217–222, Jul. 2002.
[21] L. G. Herrmann, T. Delattre, P. Morfin, J.-M. Berroir, B. Placais, D. C. Glattli, and T. Kontos, "Shot noise in Fabry–Perot interferometers based on carbon nanotubes," *Phys. Rev. Lett.*, vol. 99, no. 15, p. 156 804, Oct. 2007.
[22] H. H. Park, S. Jin, Y. J. Park, and H. S. Min, "Quantum simulation of noise in silicon nanowire transistors," *J. Appl. Phys.*, vol. 104, no. 2, p. 023 708, Jul. 2008.
[23] H. H. Park, S. Jin, Y. J. Park, and H. S. Min, "Quantum simulation of noise in silicon nanowire transistors with electron–phonon interactions," *J. Appl. Phys.*, vol. 105, no. 2, p. 023 712, Jan. 2009.
[24] M. Büttiker, "Scattering theory of current and intensity noise correlations in conductors and wave guides," *Phys. Rev. B, Condens. Matter*, vol. 46, no. 19, pp. 12 485–12 507, Nov. 1992.
[25] T. Martin and R. Landauer, "Wave-packet approach to noise in multichannel mesoscopic systems," *Phys. Rev. B, Condens. Matter*, vol. 45, no. 4, pp. 1742–1755, Jan. 1992.
[26] S. Datta, *Electronic Transport in Mesoscopic Systems*. Cambridge, U.K.: Cambridge Univ. Press, 1995.
[27] A. Betti, G. Fiori, and G. Iannaccone,*Statistical Theory of Shot Noise in Quasi-1D Field Effect Transistors in the Presence of Electron–Electron Interaction*, 2009. [Online]. Available: http://arxiv.org/abs/0904.4274
[28] A. van der Ziel, *Noise in Solid State Device and Circuits*. New York: Wiley, 1986, pp. 75–78. p. 16.
[29] *Code and Documentation*. [Online]. Available: http://www.nanohub.org/tools/vides
[30] A. Betti, G. Fiori, and G. Iannaccone, "Shot noise in quasi one-dimensional FETs," in *IEDM Tech. Dig.*, 2008, pp. 185–188.
[31] G. Fiori and G. Iannaccone, "Coupled mode space approach for the simulation of realistic carbon nanotube field-effect transistors," *IEEE Trans. Nanotechnol.*, vol. 6, no. 4, pp. 475–479, Jul. 2007.
[32] J. Guo, S. Datta, M. Lundstrom, and M. P. Anantam, "Towards multi-scale modeling of carbon nanotube transistors," *Int. J. Multiscale Comput. Eng.*, vol. 2, p. 257, 2004.
[33] G. Fiori and G. Iannaccone, "Three-dimensional simulation of one-dimensional transport in silicon nanowire transistors," *IEEE Trans. Nanotechnol.*, vol. 6, no. 5, pp. 524–529, Sep. 2007.
[34] J. Wang, E. Polizzi, and M. Lundstrom, "A three-dimensional quantum simulation of silicon nanowire transistors with the effective-mass approximation," *J. Appl. Phys.*, vol. 96, no. 4, pp. 2192–2203, Aug. 2004.
[35] G. Fiori, G. Iannaccone, and G. Klimeck, "A three-dimensional simulation study of the performance of carbon nanotube field-effect transistors with doped reservoirs and realistic geometry," *IEEE Trans. Electron Devices*, vol. 53, no. 8, pp. 1782–1788, Aug. 2006.
[36] A. A. Abidi, "High-frequency noise measurements on FETs with small dimensions," *IEEE Trans. Electron Devices*, vol. ED-33, no. 11, pp. 1801–1805, Nov. 1986.
[37] R. Navid and R. W. Dutton, "The physical phenomena responsible for excess noise in short-channel MOS devices," in *IEDM Tech. Dig.*, 2002, pp. 75–78.
[38] K. Han, H. Shin, and K. Lee, "Analytical drain thermal noise current model valid for deep submicron MOSFETs," *IEEE Trans. Electron Devices*, vol. 51, no. 2, pp. 261–269, Feb. 2004.
[39] O. M. Bulashenko and J. M. Rubí, "Shot-noise suppression by Fermi and Coulomb correlations in ballistic conductors," *Phys. Rev. B, Condens. Matter*, vol. 64, no. 4, p. 045 307, Jul. 2001.

Alessandro Betti received the B.S. and M.S. degrees in physics from the Università di Pisa, Pisa, Italy, in 2004 and 2007, respectively. He is currently working toward the Ph.D. degree in electrical engineering in the Dipartimento di Ingegneria dell'Informazione: Elettronica, Informatica, Telecomunicazioni, Università di Pisa.

Gianluca Fiori received the degree in electrical engineering and the Ph.D. degree from the Università di Pisa, Pisa, Italy, in 2001 and 2005, respectively.

In autumn 2002, he was with Silvaco International, developing quantum models, which are currently implemented in the commercial simulator ATLAS by Silvaco. In summer 2004, 2005, and 2008, he visited Purdue University, West Lafayette, IN, where he worked on models for the simulation of transport in nanoscaled devices. Since December 2007, he has been an Assistant Professor with the Dipartimento di Ingegneria dell'Informazione: Elettronica, Informatica, Telecomunicazioni, Università di Pisa. His main field of activity includes the development of models and codes for the simulations of ultrascaled semiconductor devices.

Giuseppe Iannaccone (M'98) received the M.S. and Ph.D. degrees in electrical engineering from the Università di Pisa, Pisa, Italy, in 1992 and 1996, respectively.

In 1996, he was a Researcher with the Italian National Research Council. In the same year, he became an Assistant Professor with the Dipartimento di Ingegneria dell'Informazione: Elettronica, Informatica, Telecomunicazioni, Università di Pisa, where he has been an Associate Professor in electronics since January 2001. His research interests include transport and noise in nanoelectronic and mesoscopic devices, development of device modeling and TCAD tools, and the design of extremely low power circuits and systems for RFID and ambient intelligence scenarios. He is the author or a coauthor of more than 120 papers published in peer-reviewed journals and more than 80 papers in proceedings of international conferences. He is the founder of the University spinoff company Quantavis s.r.l.

Dr. Iannaccone has coordinated a few European and National Projects involving multiple partners and has acted as a Principal Investigator in several research projects funded by public agencies at the European and national levels and by private organizations. He is in the Technical Committee of a few international conferences and serves as a referee for the leading journals in the fields of condensed matter physics, device electronics, and circuit design.

Authorized licensed use limited to: UNIVERSITA PISA S ANNA. Downloaded on October 26, 2009 at 05:55 from IEEE Xplore. Restrictions apply.